IEEE Access
Multidisciplinary | Rapid Review | Open Access Journal

Received February 20, 2020, accepted March 5, 2020, date of publication March 10, 2020, date of current version March 19, 2020.

Digital Object Identifier 10.1109/ACCESS.2020.2979919

Fractional Order Impedance Control

GUANGRONG CHEN[1], SHENG GUO[1], BOWEN HOU[2], AND JUNZHENG WANG[3]
[1]Robotics Research Center, Beijing Jiaotong University, Beijing 100044, China
[2]Beijing Engineering and Technology Research Center of Rail Transit Line Safety and Disaster Prevention, Beijing 100044, China
[3]State Key Laboratory of Intelligent Control and Decision of Complex Systems, School of Automation, Beijing Institute of Technology, Beijing 100081, China

Corresponding author: Guangrong Chen (grchen@bjtu.edu.cn)

This work was supported in part by Fundamental Research Funds for the Central Universities under Grant 2019JBM051, in part by the Beijing Engineering and Technology Research Center of Rail Transit Line Safety and Disaster Prevention Open Foundation for Research under Grant RRC201701, in part by the Beijing Natural Science Foundation under Grant 3204051, and in part by the Ministry of Science and Technology of the People's Republic of China under Grant 2017YFB1201104.

ABSTRACT This paper proposes a novel fractional order impedance control. In traditional impedance control model, the orders of inertia, damping, and stiffness are integers and the contact force can be reduced effectively to some extent in robots and manipulators. However, there exists a tracking error of end-effector at the stable state due to the existence of stiffness, which is not conducive to tackle tasks based on high performance position control for robots and manipulators. Thus, an integral item is added into the traditional impedance model to eliminate the tracking error. Besides, the idea of fractional order is introduced to make the orders of inertia, damping, and stiffness change from integers to fractions to achieve more significant compliant performance. Simulation results validate the advantages of proposed fractional order impedance control and it can be also employed to absorb/increase, hold/keep, and dissipate/decrease system energy to achieve jumping, bouncing and friendly contact, respectively. Also, three criterions of choosing and tuning all these 14 parameters in the proposed fractional order impedance control are given out. This provides an insight for robot dynamic interaction, bouncing and jumping control.

INDEX TERMS Fractional order, impedance control, compliance control, dynamic interaction.

I. INTRODUCTION

Robots are expected to be employed for a variety of tasks involving interaction with dynamic environments, like material transportation, geographic expedition and disaster rescue etc [1]. In these cases, the environmental terrains are normally unstructured or unknown and robots should confront with impacts and crashes when negotiating the contact. Traditional position servo control is with high gain (stiffness) and usually in kinematic control, which makes the robots rigid and increases the contact force. A good solution to deal with the impact is making the end-effector of robots work like a spring-damper [2], while the stiffness and damping should be variable with respect to time, terrains and tasks [3], [4].

Compliance control is an effective way to detail with robotic environmental interaction [5], [6]. Compliance can be passive and active. Passive compliance can be implemented easily by a spring. Generally, the spring stiffness is fixed. And several actuators with variable stiffness can not consider the weight (load mass), volume (length limitation), complexity, and velocity saturation (motion frequency) etc at the same time [7], [8]. However, Shen Z H and Seipel J proposed the variable leg stiffness animals use in different motions may improve the stability of locomotion [9] and reduce the energetic cost of locomotion [10]. Most importantly, passive spring cannot dissipate impact energy due to its less damping [11]. If the damping is added into a special designed spring-damper-like device, its impedance cannot be tuned flexibly as well [12]. Thus, passive compliance can be an auxiliary but not the main way to achieve compliance control. Considering active compliance [13], there are two ways to realize it: force control and impedance control [14]–[17]. The active compliance based on force control is also called position/force control or admittance control [18], [19], which consists of hybrid position/force control [20]–[22] and unified position/force control [23]–[25]. The active compliance based on impedance control can be also divided into two kinds: based on position and based on force [26], [27]. In robot systems, being compliant to external unexpected impacts is crucial when

The associate editor coordinating the review of this manuscript and approving it for publication was Norbert Herencsar.

negotiating unstructured environments. Compliance control based on force control is an ideal choice for its flexibility of designing the contact impedance. However, this method requires a high performance force control and a precise dynamics model [28]. Comparing with that based on force, the compliant behavior based on position control, which has been also studied for many years [7], is easier to implement in practical use.

To be more friendly with the environment, robots should be set to be task-based and flexible in stiffness and damping because of the changing loads, environments, and tasks. But as for the traditional impedance model [7], as long as an external force is added on the end-effector of robot, there exists a tracking error at the end-effector, which will affect the stability of robot with different loads and environments or the operation accuracy of robot with different tasks. Besides, the transition performance of robot between position and force is not good enough for dynamic interactions in the traditional impedance model since its orders of inertia, damping, and stiffness are integers, but not fractions like that in fractional order PID control [29]. Therefore, an integral item is added into the traditional impedance model to eliminate the tracking error. And then, the idea of fractional order is introduced to make the orders of inertia, damping, and stiffness change from integers to fractions to achieve more significant compliant performance, like the difference between traditional PID and fractional order PID. Even though the realization of fractional order impedance by feedback control has been presented by Oh Sehoon and Hori Yoichi in literature [30], [31], there still exists a big difference from the proposed method in this paper. The fractional order impedance in literature [30], [31] is based on velocity control and the fractional order only appears on the stiffness part. However, the proposed fractional order impedance control has a novel and different format, which is based on more popular position control and the fractional order appears all over the model including inertia, damping, and stiffness etc [32]. In addition, the proposed fractional order impedance control also adds an integral item to eliminate the tracking error, this paper also gives out three criterions of choosing and tuning all these 14 parameters in the proposed fractional order impedance control, and other different functions of the proposed fractional order impedance control on the system energy: absorb/increase, hold/keep, and dissipate/decrease, are also analyzed for clear.

In the system modelling and controller designing, fractional-order has been validated as a significant technique to improve the performance of system [33], [34]. The drawbacks of PID control schemes have been overcome to a large extent by fractional-order PID (FOPID) controllers. FOPID control schemes can be represented by $PI^{\lambda}D^{\mu}$, where the values of λ and μ are both fractional orders. While PID controllers include only integer-order operators. The introduction of λ and μ makes the controller design more flexible and enhances the performance of controller [35]. Many efforts have represented definitions for fractional-order operators [29], [36]–[40]. Richard Herrmann presented an introduction of fractional calculus for physicists, which is devoted to the application of fractional calculus on physical problems [36]. Manuel Duarte Ortigueira presented the fractional calculus for scientists and engineers and gave a practical overview of fractional calculus as it relates to signal processing [37]. Richard Magin presented the fractional calculus in bioengineering for bioengineers who wish to learn more about fractional calculus and the ways in which it can be used to solve biomedical problems [38]. Moreover, Duarte Valério and José Sá Da Costa presented an introduction to fractional control, which outlines the theory, techniques and applications of fractional control [29]. Concepción Monje and his research group detail the use of fractional calculus in the description and modeling of systems, and in a range of control design and practical applications [39]. Hadi Delavari and his research group studied an intelligent robust fractional surface sliding mode control for a nonlinear system [40]. In theory, $PI^{\lambda}D^{\mu}$ is an infinite dimensional linear filter, as the order of the integrator and differentiator is fractional [35]. Therefore, the fractional-order operators could be approximated by equivalent finite dimensional transfer functions. There are various studies on obtaining a realizable form for s^{μ} [41]. For instance, Oustaloup et al introduced a powerful method for the realization of s^{μ} using the recursive distribution of zeros and poles [42].

In fact, the robotic leg can be equivalent to a bouncing system or hopper [43], which behaves like a mass-spring-damper system [44]. To analyze the impedance performance of robotic leg directly is complicated, but it simple to discuss the one of a hopper [45]. Also, due to the high accuracy [46], fast response [47] and strong load capacity [48] of hydraulic actuator [49], [50], it has been a good choice for robotic actuator [51]. Hence, a hydraulic bouncing system was chosen as a research subject.

The main contributions are concluded as follows:

- An integral item is added into the traditional impedance model to eliminate the tracking error caused by the compliant behavior.
- The idea of fractional order is introduced to make the orders of inertia, damping, and stiffness are no longer only integers so that more significant compliant performance can be achieved.
- The proposed novel fractional order impedance control is validated by comparative simulations in a hydraulic bouncing system and three criterions of choosing and tuning all these 14 parameters in the proposed fractional order impedance control are given out.

In this paper, a novel fractional order impedance control is proposed and validated. The paper is organized as follows. In *Section* II, the simulation model of a hydraulic bouncing system is given out. In *Section* III, the mathematical foundations of fractional order and traditional impedance control are addressed, and the novel fractional order impedance control is proposed, which combines the fractional order and an integral item into the traditional impedance control. In *Section* IV,

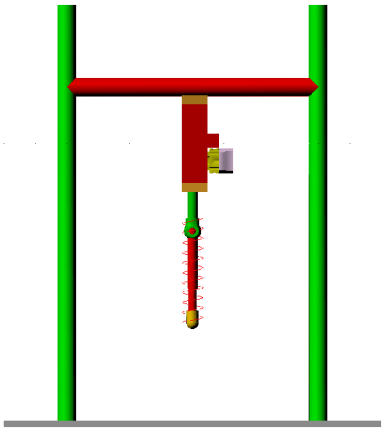

FIGURE 1. The hydraulic bouncing system.

TABLE 1. System parameters.

Supply pressure	120bar
Stroke of cylinder	76mm
Diameter of cylinder piston	25mm
Diameter of cylinder rod	16mm
Flow rate of servo valve	16L/min
Response frequency of servo valve	120Hz
Lumped mass of system M	16.83kg
Stiffness of spring K_s	40N/mm
Damping of spring D_s	0.05Ns/mm
Initial falling height H	160mm

the parameters of proposed fractional order impedance model are analyzed and comparative simulations are implemented to validate the compliant behavior of proposed fractional order impedance model. In *Section* V, conclusions are drawn and future work is issued.

II. SYSTEM MODEL

Compliance control makes sense for solving how to accomplish the friendly contact with less impact between robots and environment [1]. In fact, the most important problem in compliance control is looking for an equilibrium point between position control and contact force. Moreover, a robotic leg can be regarded as a hydraulic bouncing system to simplify the research. Therefore, our research subject is a hydraulic bouncing system in Adams software, as shown in Fig. 1. This system includes: a position controllable cylinder for active compliance control and a built-in passive spring for passive compliance. Note that the hydraulic bouncing system is one-dimensional and constrained to move in the vertical direction. In this system, how to deal with the impact contact in free falling, bouncing and jumping by compliance control can be issued and it will provide an insight for the compliance control for legged robots. The basic system parameters are shown in Table 1.

Compared with the compliant pneumatic drive in position servo control [52], the traditional hydraulic drive is rigid, as shown in Fig. 2(a), where M is the lumped mass of the

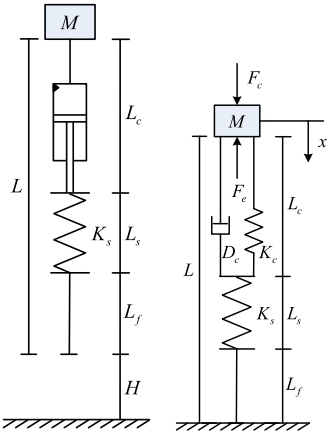

(a) The equivalent system of hydraulic bouncing system (b) The equivalent model of hydraulic bouncing system

FIGURE 2. The equivalent system.

system; L, L_c, L_s, L_f and H are respectively the total length of hydraulic bouncing system, the length of cylinder, the length of spring, the length of foot and the free falling height; K_s is the stiffness of passive spring, which can be taken as the stiffness of environment ($\frac{K_e K_s}{K_e+K_s}$) for the cylinder when the touch terrain is rigid, which means $K_e = \infty$. The stiffness of hydraulic cylinder in the position servo control is so large that it can be omitted. Thus, the stiffness of the whole system only depends on the built-in passive spring. In order to prevent the over compression of passive spring, the stiffness of the spring is chosen to be large enough, which will lead to a large contact impact. In addition, the damping in the position servo control of hydraulic cylinder is mainly decided by the frictional damping and throttle damping, which are so small that the cylinder will undergo low damping oscillations.

The active compliance control can be seen as a balance between position servo control and force control, which makes the position servo control change from rigid to compliant by redesigning a impedance controller and adding force sensing into it, and results in reducing the contact impact and oscillations. As shown in Fig. 2(b), the stiffness and damping of active compliance can be set and controlled at the same time, where x is the displacement of lumped mass; K_c, D_c is the actual stiffness and damping of hydraulic cylinder system, respectively; F_c is the control force produced by hydraulic cylinder; F_e is the contact impact force, which almost equals to the force $F_s = K_s \Delta L_s$, produced by passive spring when the spring has a small mass and damping, where ΔL_s represents the compression of passive spring caused by contact impact.

Actually, the dynamic equation of lumped mass can be easily written as

$$M(\ddot{x} + g) = F_c - F_e \tag{1}$$

where g is the gravitational acceleration.

Without loss of generality, a more common dynamic equation with n dimensions is taken into consideration, which can be described by

$$\boldsymbol{M}\ddot{\boldsymbol{x}} + \boldsymbol{C}\dot{\boldsymbol{x}} + \boldsymbol{G} = \boldsymbol{F}_c - \boldsymbol{F}_e = \boldsymbol{F}^* \tag{2}$$

where $\boldsymbol{M} \in \mathbb{R}^{n\times n}$ denotes the mass matrix; $\boldsymbol{C} \in \mathbb{R}^{n\times n}$ denotes the matrix of Coriolis and centrifugal terms; $\boldsymbol{G} \in \mathbb{R}^n$ denotes the gravity terms; $\boldsymbol{F}^*, \boldsymbol{F}_c, \boldsymbol{F}_e \in \mathbb{R}^n$ donate the net, control and environmental force/moment vector of rigid body, respectively.

The compliance control was designed and the stability analysis was issued as follows to obtain a better compliance control performance without losing the accuracy of position control.

III. FRACTIONAL ORDER IMPEDANCE CONTROL

The novel fractional order impedance control combining the fractional order and an integral item is proposed in *Section* III-C. The mathematical foundations for fractional order and traditional impedance control are firstly given out in *Section* III-A and III-B, respectively.

A. FRACTIONAL ORDER

The family of PID controllers is a well-known type of linear controllers used in many industrial applications. In PID controllers, each of proportional, derivative and integral gains plays a specific role in controlling a system. For example, a proportional gain is used to reduce the rise time and decrease the steady state error in time domain response of a system. A derivative gain is useful for increasing the stability and reducing the overshoot; however, it amplifies the high frequency noise. Finally, the integral gain is utilized to eliminate the steady state error, but makes the transient response worse. FOPID schemes have been introduced to improve the overall performance of the system compared with PID controllers. The overall structure of a FOPID controller is given by

$$C_{FOPID} = K_P + K_I s^{-\lambda} + K_D s^{\mu} \tag{3}$$

As seen from (3), there are two more tuning parameters in FOPID scheme ($PI^{\lambda}D^{\mu}$) as compared with PID controllers. λ and μ are positive and real numbers. In fact, they have been added into the classical PID controllers to make a compromise between the pros and cons of the integer-order integral and derivative parts, and make the controller design more flexible. There are many methods to do the fractional calculus. Richard Magin and his research group have done a look into fractional calculus and its applications from the signal processing point of view and presented a coherent approach to the fractional derivative [53]. Manuel Ortigueira and José Machado discussed the actual state of interplay between fractional calculus, signal processing, and applied sciences and described a framework for compatible integer and fractional derivatives/integrals in signals and systems context [54]. But those are not the main point here. The importance is the improved performances of proposed fractional order impedance control. In this paper, the Oustaloup recursive approach is used as the approximation method of fractional calculus. According to the Oustaloup [42], a fractional-order operator can be approximated by a fraction comprising a number of real zeros and poles.

Fractional-order differentiators and integrators are the generalized version of integer-order operators. In fractional calculus, the fractional-order differentiation and integration operators are usually shown by D^{α} and J^{α}, respectively [55]. Extensive explanations on the definitions of fractional-order operators have been presented in many literatures [29], [36]–[40]. In integer-order calculus, the term α has a positive and integer value, while it is a positive and real value in fractional-order calculus.

The output of a non-integer differentiator, in time domain, can be expressed generally as [42]

$$y(t) = \tau^{\alpha}\left(\frac{d}{dt}\right)^{\alpha} x(t) \tag{4}$$

where τ is a real and positive time constant. If (4) is translated to s domain, then [42]

$$Y(s) = \left(\frac{s}{\omega_u}\right)^{\alpha} X(s) \tag{5}$$

where ω_u is called as the unit frequency gain, and $\omega_u = \frac{1}{\tau}$. Based on (5), the non-integer order transmittance $D(s)$ is defined as [42]

$$D(s) = \left(\frac{s}{\omega_u}\right)^{\alpha} \tag{6}$$

To cut-off both high and low frequencies, the differentiation transfer function $\frac{s}{\omega_u}$ can be limited to a given frequency range $[\omega_L, \omega_H]$, and is replaced by the following frequency-bounded differentiation transfer function [42]

$$\frac{s}{\omega_u} \cong W\frac{1 + s/\omega_l}{1 + s/\omega_h} \tag{7}$$

such that,

$$\begin{cases} \omega_u = \sqrt{\omega_l \omega_h} \\ W = \dfrac{\omega_l}{\omega_u} = \dfrac{\omega_u}{\omega_h} \end{cases} \tag{8}$$

In (7), ω_l and ω_h denote the low- and high-transitional frequencies, and,

$$\begin{cases} \omega_l \leqslant \omega_L \\ \omega_h \geqslant \omega_H \end{cases} \tag{9}$$

Combining (5) to (9), the fractional-order transmittance $D(s)$ is expressed as [42]

$$D(s) = \left(\frac{\omega_u}{\omega_h}\right)^{\alpha}\left(\frac{1 + s/\omega_l}{1 + s/\omega_h}\right)^{\alpha} \tag{10}$$

In order to approximate $D(s)$ by an equivalent finite dimensional transfer function, a recursive distribution of real poles and zeros is used such that [42]

$$D(s) = \lim_{N\to\infty} D_N(s) \tag{11}$$

where,

$$D_N(s) = \left(\frac{\omega_u}{\omega_h}\right)^{\alpha} \prod_{k=-N}^{N} \frac{1 + s/\omega'_l}{1 + s/\omega'_h} \tag{12}$$

and, ω'_l and ω'_h are defined as [42]

$$\begin{aligned} \omega'_l &= \omega_l \left(\frac{\omega_h}{\omega_l}\right)^{\frac{k+N+\frac{1-\alpha}{2}}{2N+1}} \\ \omega'_h &= \omega_l \left(\frac{\omega_h}{\omega_l}\right)^{\frac{k+N+\frac{1+\alpha}{2}}{2N+1}} \end{aligned} \tag{13}$$

Selection of N leads to the determination of $D_N(s)$ from Eq. (18). Therefore, $D_N(s)$ is an integer-order transfer function approximating the fractional-order differentiator $D(s) = \left(\frac{s}{\omega_u}\right)^{\alpha}$. Note that $D_N(s)$ consists of $2N + 1$ numbers of zeros or poles. With respect to the available hydraulic system, $N = 2$ was sufficient to obtain a good approximation for the fractional-order operators. Considering greater values for N will result in the generation of excessive poles and zeros in $D_N(s)$. Since this paper focus on fractional order, the details about parameters tuning and stability analysis of FOPID, which can be found in [30], [56]–[59], is omitted here.

B. IMPEDANCE CONTROL

To improve the motion stability of legged robots and decrease the contact impact on the foot, the robotic legs should be compliant. The compliance includes passive and active compliance. Generally, passive compliance can be obtained by configuring the foot with a spring-damper. However, due to the limitation of the length of spring, the stiffness of spring can not be too small to be a part or too large to reduce the contact impact effectively. In addition, the values of stiffness and damping of spring-damper are preselected and can not change with different loads and terrains, which will lead to body oscillations since the load mass mismatch with the fixed stiffness and damping [7].

To solve the problems, active compliance was introduced into position servo control of hydraulic cylinder to make the stiffness and damping controllable. The objective of active compliance control is to reduce the high contact impedance (stiffness) of position servo control of mechanical system by controlling the external contact force of dynamic interaction. If the environment is regarded as a source of disturbance, then modulating the disturbance response of robots will permit the control of dynamic interaction [7]. In this subsection, the position/force based compliance controller was introduced firstly, then the compliance control was employed to address the hydraulic bouncing system.

There are two basic ways to achieve active compliance control, one is position-mode with an outer force loop and the other is force-mode with an inner force loop [1]. Force-based compliance control is mainly applied in robotic systems with a relatively good causality between joint actuator torques and

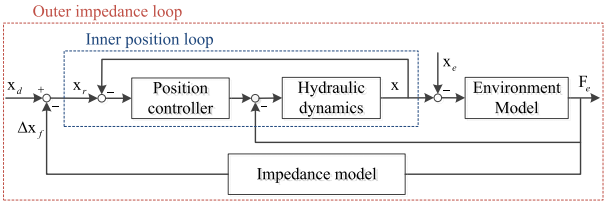

FIGURE 3. The diagram of position/force based active compliance controller.

end-effector forces. On the contrary, position-based compliance control is easier and more reliable for hydraulic actuated robots since it does not require accurate dynamics model of robot and high performance force control. Thus, the diagram of position/force based active compliance controller is illustrated in Fig. 3, where $\boldsymbol{x}_d, \boldsymbol{x}, \boldsymbol{x}_r, \boldsymbol{x}_e \in \mathbb{R}^n$ donates the desired displacement, actual displacement, required displacement, and the displacement caused by the environment, respectively. The impedance model is utilized to shape the relationship between contact force $\boldsymbol{F}^*$ and corresponding nominal position modifications or output of target admittance $\Delta\boldsymbol{x}_f \in \mathbb{R}^n$. And there exist an inner position loop and an outer impedance loop.

The dynamic operator that determines an input force ($\boldsymbol{F}_e$) from an output velocity ($\dot{\boldsymbol{x}}$) of the end-effector at the interaction port is defined as the mechanical driving-point admittance (Y), which is defined as the inverse of the impedance (Z) on the other hand and can be written as

$$\dot{\boldsymbol{x}} = Y(s)\boldsymbol{F}_e = Z^{-1}(s)\boldsymbol{F}_e \tag{14}$$

Considering (14), the necessary and sufficient conditions for passivity of a linear time invariant multi-port system are as follows [8]. That is, $Y(s)$ is passive if and only if:

- $Y(s)$ has no pole in right-half plane $\Re(s) > 0$;
- $Y(s) + Y^*(s)$ is positive semi-definite in $\Re(s) > 0$, where $Y^*(s)$ is the conjugate transpose of $Y(s)$.

When $Y(s)$ has no poles in $\Re(s) \geq 0$, then the second condition can be simplified to:

- The matrix $Y(j\omega) + Y^*(j\omega)$ is positive semi-definite for all real ω.

In compliance control, one control objective is to make the actual displacement track the required displacement. A required displacement differs from a desired displacement, as it can include one or more terms related to control errors. The required displacement vector $\boldsymbol{x}_r$, expressed in the Cartesian coordinates [60], is written as

$$\boldsymbol{x}_r = \boldsymbol{x}_d + \boldsymbol{\Gamma}_D(\dot{\boldsymbol{x}}_d - \dot{\boldsymbol{x}}) + \boldsymbol{\Gamma}_M(\ddot{\boldsymbol{x}}_d - \ddot{\boldsymbol{x}}) + \boldsymbol{\Gamma}_F(\boldsymbol{F}_d - \boldsymbol{F}_e) \tag{15}$$

where $\boldsymbol{F}_d$ is the desired vector of environmental force/moment vector; $\boldsymbol{\Gamma}_D, \boldsymbol{\Gamma}_M, \boldsymbol{\Gamma}_F \in \mathbb{R}^{n\times n}$ are three diagonal positive-definite matrices, characterizing Cartesian velocity, acceleration, and force control, respectively.

Note that there exists the term $\boldsymbol{F}_d - \boldsymbol{F}_e$ in (15). According to [7], the target impedance for the model can be described as

$$\boldsymbol{F}_d - \boldsymbol{F}_e = -\boldsymbol{K}(\boldsymbol{x}_d - \boldsymbol{x}) - \boldsymbol{D}(\dot{\boldsymbol{x}}_d - \dot{\boldsymbol{x}}) - \boldsymbol{M}(\ddot{\boldsymbol{x}}_d - \ddot{\boldsymbol{x}}) \quad (16)$$

where $\boldsymbol{K}, \boldsymbol{D}, \boldsymbol{M} \in \mathbb{R}^{n\times n}$ are diagonal positive-definite matrices and characterize the desired stiffness, damping and inertia, respectively. Specially, $\boldsymbol{F}_d - \boldsymbol{F}_e \neq 0$ denotes constrained motion and $\boldsymbol{F}_d - \boldsymbol{F}_e = 0$, with $\boldsymbol{F}_d$ equals a zero vector, denotes free-space motions.

In order to achieve the target impedance behavior in (16), the diagonal positive-definite matrices $\boldsymbol{\Gamma}_D, \boldsymbol{\Gamma}_M, \boldsymbol{\Gamma}_F$ in (15) can be defined as the following *Condition* 1.

Condition 1: The diagonal positive-definite matrices $\boldsymbol{\Gamma}_D, \boldsymbol{\Gamma}_M, \boldsymbol{\Gamma}_F$ can be defined as

$$\begin{aligned} \boldsymbol{\Gamma}_F &= \boldsymbol{K}^{-1} \\ \boldsymbol{\Gamma}_D &= \boldsymbol{\Gamma}_F \boldsymbol{D} \\ \boldsymbol{\Gamma}_M &= \boldsymbol{\Gamma}_F \boldsymbol{M} \end{aligned} \quad (17)$$

The following *Theorem* 1 provides that the target impedance behavior (16) can be achieved for the system.

Theorem 1: Consider the required displacement behavior for the system in (15). If and only if the diagonal positive-definite matrices $\boldsymbol{\Gamma}_D, \boldsymbol{\Gamma}_M, \boldsymbol{\Gamma}_F$ are defined according to (17) in *Condition* 1, then the required displacement behavior (15) equals the target impedance behavior (16).

Proof: Substituting (16) into (15) and using *Condition* 1 yields

$$\begin{aligned} \boldsymbol{x}_r &= \boldsymbol{x}_d + \boldsymbol{\Gamma}_D(\dot{\boldsymbol{x}}_d - \dot{\boldsymbol{x}}) + \boldsymbol{\Gamma}_M(\ddot{\boldsymbol{x}}_d - \ddot{\boldsymbol{x}}) \\ &\quad + \boldsymbol{\Gamma}_F(-\boldsymbol{K}(\boldsymbol{x}_d - \boldsymbol{x}) - \boldsymbol{D}(\dot{\boldsymbol{x}}_d - \dot{\boldsymbol{x}}) - \boldsymbol{M}(\ddot{\boldsymbol{x}}_d - \ddot{\boldsymbol{x}})) \\ &= \boldsymbol{x}_d + \boldsymbol{\Gamma}_F\boldsymbol{D}(\dot{\boldsymbol{x}}_d - \dot{\boldsymbol{x}}) + \boldsymbol{\Gamma}_F\boldsymbol{M}(\ddot{\boldsymbol{x}}_d - \ddot{\boldsymbol{x}}) \\ &\quad - \boldsymbol{\Gamma}_F\boldsymbol{K}(\boldsymbol{x}_d - \boldsymbol{x}) + \boldsymbol{\Gamma}_F(-\boldsymbol{D}(\dot{\boldsymbol{x}}_d - \dot{\boldsymbol{x}}) - \boldsymbol{M}(\ddot{\boldsymbol{x}}_d - \ddot{\boldsymbol{x}})) \\ &= \boldsymbol{x}_d - \boldsymbol{K}^{-1}\boldsymbol{K}(\boldsymbol{x}_d - \boldsymbol{x}) \\ &= \boldsymbol{x} \end{aligned} \quad (18)$$

Then, using *Condition* 1 and (18) yields

$$\begin{aligned} &\boldsymbol{F}_d - \boldsymbol{F}_e\mathcal{D} - \boldsymbol{\Gamma}_F^{-1}(\boldsymbol{x}_d - \boldsymbol{x}_r) - \boldsymbol{\Gamma}_F^{-1}\boldsymbol{\Gamma}_D(\dot{\boldsymbol{x}}_d - \dot{\boldsymbol{x}}) \\ &\quad - \boldsymbol{\Gamma}_F^{-1}\boldsymbol{\Gamma}_M(\ddot{\boldsymbol{x}}_d - \ddot{\boldsymbol{x}}) \\ &= -\boldsymbol{K}(\boldsymbol{x}_d - \boldsymbol{x}_r) - \boldsymbol{\Gamma}_F^{-1}\boldsymbol{\Gamma}_F\boldsymbol{D}(\dot{\boldsymbol{x}}_d - \dot{\boldsymbol{x}}) - \boldsymbol{\Gamma}_F^{-1}\boldsymbol{\Gamma}_F\boldsymbol{M}(\ddot{\boldsymbol{x}}_d - \ddot{\boldsymbol{x}}) \\ &= -\boldsymbol{K}(\boldsymbol{x}_d - \boldsymbol{x}) - \boldsymbol{D}(\dot{\boldsymbol{x}}_d - \dot{\boldsymbol{x}}) - \boldsymbol{M}(\ddot{\boldsymbol{x}}_d - \ddot{\boldsymbol{x}}) \end{aligned} \quad (19)$$

Note that the first row in (19) is equal to (15), whereas the last row is equal to (16). This completes the proof for *Theorem* 1.

The desired impedance $Z_f(s)$ is usually adopted in the form of second-order linear system (spring-damping-inertia system) [7]:

$$Z_f(s) = \frac{1}{\boldsymbol{M}s^2 + \boldsymbol{D}s + \boldsymbol{K}} \quad (20)$$

Noting that $'D'$ could be derivative-related or damping-related. Please follow its context to distinguish the difference.

C. A NOVEL FRACTIONAL ORDER IMPEDANCE CONTROL

Based on (16), consider a more common relationship between the interface force F_e and tracking error $\Delta x = x_d - x$ of end-effector with respect to time as

$$\begin{aligned} &D_{x_{md}}\Delta x^{(d_{x_{md}})}(t) + D_{x_{md-1}}\Delta x^{(d_{x_{md-1}})}(t) + \cdots \\ &\quad + D_{x_2}\Delta x^{(d_{x_2})}(t) + D_{x_1}\Delta x^{(d_{x_1})}(t) + K_x\Delta x(t) \\ &\quad + I_{x_1}\left(\int\right)^{i_{x_1}}\Delta x(t)dt + I_{x_2}\left(\int\right)^{i_{x_2}}\Delta x(t)dt + \cdots \\ &\quad + I_{x_{mi-1}}\left(\int\right)^{i_{x_{mi-1}}}\Delta x(t)dt + I_{x_{mi}}\left(\int\right)^{i_{x_{mi}}}\Delta x(t)dt \\ &= D_{f_{nd}}F_e^{(d_{f_{nd}})}(t) + D_{f_{nd-1}}F_e^{(d_{f_{nd-1}})}(t) + \cdots \\ &\quad + D_{f_2}F_e^{(d_{f_2})}(t) + D_{f_1}F_e^{(d_{f_1})}(t) + K_fF_e(t) \\ &\quad + I_{f_1}\left(\int\right)^{i_{f_1}}F_e(t)dt + I_{f_2}\left(\int\right)^{i_{f_2}}F_e(t)dt + \cdots \\ &\quad + I_{f_{ni-1}}\left(\int\right)^{i_{f_{ni-1}}}F_e(t)dt + I_{f_{ni}}\left(\int\right)^{i_{f_{ni}}}F_e(t)dt \end{aligned} \quad (21)$$

where $D_{x_i}(i = 1, \ldots, md), D_{f_i}(i = 1, \ldots, nd) \in \mathbb{R}$ are the coefficients of derivative parts of $\Delta x(t)$ and $F_e(t)$, respectively. $I_{x_i}(i = 1, \ldots, mi), I_{f_i}(i = 1, \ldots, ni) \in \mathbb{R}$ are the coefficients of integral parts of $\Delta x(t)$ and $F_e(t)$, respectively. $d_{x_i}(i = 1, \ldots, md), d_{f_i}(i = 1, \ldots, nd) \in \mathbb{R}$ are the orders of derivative parts of $\Delta x(t)$ and $F_e(t)$, respectively. $i_{x_i}(i = 1, \ldots, mi), i_{f_i}(i = 1, \ldots, ni) \in \mathbb{R}$ are the orders of integral parts of $\Delta x(t)$ and $F_e(t)$, respectively. K_x, K_f are the gain coefficients of $\Delta x(t)$ and $F_e(t)$, respectively. Moreover, $0 < d_{x_1} < d_{x_2} < \cdots < d_{x_{md-1}} < d_{x_{md}}$, $0 < d_{f_1} < d_{f_2} < \cdots < d_{f_{nd-1}} < d_{f_{nd}}$, $0 < i_{x_1} < i_{x_2} < \cdots < i_{x_{mi-1}} < i_{x_{mi}}$, $0 < i_{f_1} < i_{f_2} < \cdots < i_{f_{ni-1}} < i_{f_{ni}}$. If (21) is translated to s domain, the transfer function of (21) can be written as

$$\frac{\Delta x(s)}{F_e(s)} = \frac{\begin{array}{l} D_{f_{nd}}s^{d_{f_{nd}}} + D_{f_{nd-1}}s^{d_{f_{nd-1}}} + \cdots \\ +D_{f_2}s^{d_{f_2}} + D_{f_1}s^{d_{f_1}} \\ +K_f + I_{f_1}s^{-i_{f_1}} + I_{f_2}s^{-i_{f_2}} + \cdots \\ +I_{f_{mi-1}}s^{-i_{f_{mi-1}}} + I_{f_{mi}}s^{-i_{f_{mi}}} \end{array}}{\begin{array}{l} D_{x_{md}}s^{d_{x_{md}}} + D_{x_{md-1}}s^{d_{x_{md-1}}} + \cdots \\ +D_{x_2}s^{d_{x_2}} + D_{x_1}s^{d_{x_1}} \\ +K_x + I_{x_1}s^{-i_{x_1}} + I_{x_2}s^{-i_{x_2}} + \cdots \\ +I_{x_{ni-1}}s^{-i_{x_{ni-1}}} + I_{x_{ni}}s^{-i_{x_{ni}}} \end{array}} \quad (22)$$

Noting that these parameters are all integers in traditional cases. Easy to see that this kind of impedance model based on force/position (21)(22) is complicated and with lots of parameters. But it covers every kind of situations we need in real applications, such as the traditional impedance model, the model dissipating, holding, or absorbing energy.

For simplicity, a special and useful example of (22) (the proposed novel fractional order impedance model) for legged robots is addressed as

$$\frac{\Delta x(s)}{F_e(s)} = \frac{D_{f_1}s^{d_{f_1}} + K_f + I_{f_1}s^{-i_{f_1}}}{D_{x_2}s^{d_{x_2}} + D_{x_1}s^{d_{x_1}} + K_x + I_{x_1}s^{-i_{x_1}} + I_{x_2}s^{-i_{x_2}}} \quad (23)$$

where all the coefficients and orders are larger than 0 and belong to real number (no longer only integers). Specially,

$0 < d_{x_1} < 1.5 \leqslant d_{x_2} \leqslant 2.5, 0 < i_{x_1} < 1.5 \leqslant i_{x_2} \leqslant 2.5$. By comparison, D_{x_2}, D_{x_1} and K_x are the set impedance-like inertia, damping, stiffness as in (16). The integral item in the denominator of (23) is utilized to eliminate the tracking error in traditional impedance model, while the integral item in the numerator of (23) is utilized to increase the tracking error in traditional impedance model. The derivative item in the numerator of (23) is used to absorb/increase the system energy, while the derivative item in the denominator of (23) is used to dissipate/decresase the system energy.

Although there are still 14 parameters in (23), it is more simple and acceptable than (22).

IV. SIMULATION ANALYSIS

Based on the proposed novel fractional order impedance model in (23), co-simulations are done between Adams software and Matlab. Adams is a multibody dynamics simulation software, which is used to build up the virtual prototypes of hydraulic bouncing system model as shown in Fig. 1. Matlab is used to design the position/force based active compliance controller as shown in Fig. 3 and achieve the proposed fractional order impedance model (23) in the diagram via Oustaloup's method in literature [42]. The simulation parameters are the same to Table 1. All the simulations start with the same initial falling height $H = 160mm$, but with different impedance models. Firstly, the influence of each parameter on the relationship between contact force and system tracking error of end-effector is analyzed. Then, comparative simulations are implemented to validate the compliant behavior of proposed impedance model. Finally, three criterions of choosing and tuning all these 14 parameters in (23) are figured out.

A. THE INFLUENCE OF EACH PARAMETER

There are two main problems in designing a FOPID controller experimentally: (i) an approximation method is required to realize the fractional-order differentiators and integrators, and (ii) an optimization algorithm is needed for the control parameters tuning based on the experimental data. The first problem can be solved in *Section* III-A via Oustaloup's method [42]. Through comparing six different values of one of the 14 parameters in a given model, the analyzed effects of every parameter are shown in Fig. 4.

The functions of parameters in the chosen models are concluded as follows:

1) Model 1: $\frac{1}{D_{x_1}s^1+10}$
   D_{x_1} is the traditional damping in (16). A large D_{x_1} can dissipate the system energy and reduce the oscillations, but it will increase the contact force in turn.
2) Model 2: $\frac{1}{0.6s^{d_{x_1}}+10}$
   When d_{x_1} closes to 1.5, the damping-like D_{x_1} begins to behave inertia-like, which results in the growing contact force and oscillations before the system comes into a stable state. When d_{x_1} closes to 0, D_{x_1} begins

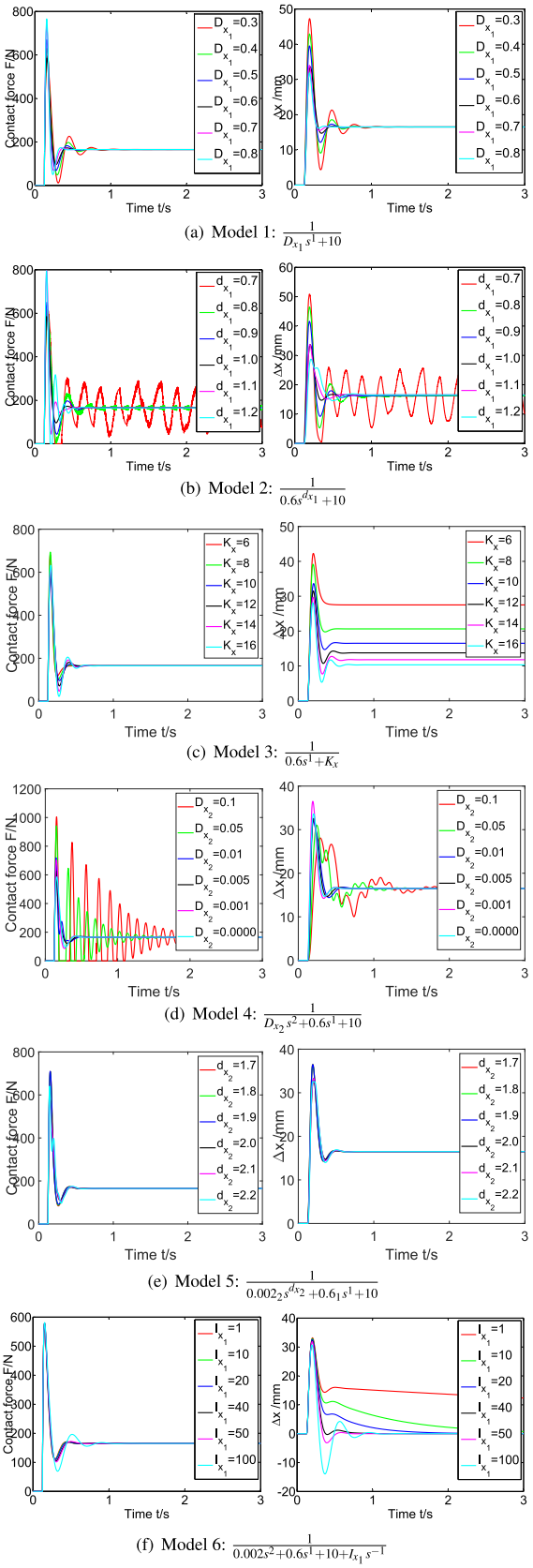

FIGURE 4. The influences of parameters in (23): Model 1∼5.

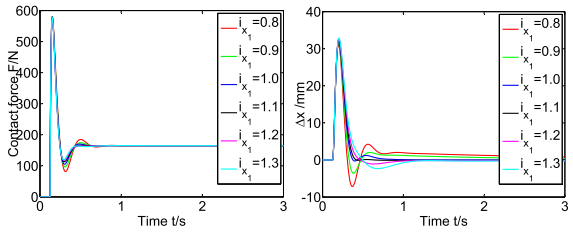

(g) Model 7: $\frac{1}{0.002s^2+0.6s^1+10+40s^{-ix_1}}$

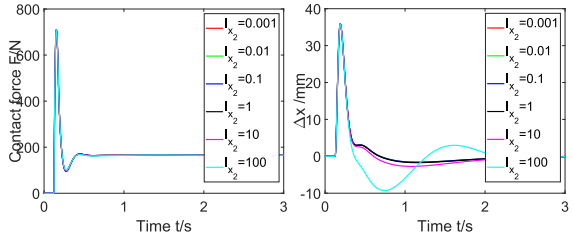

(h) Model 8: $\frac{1}{0.002s^2+0.6s^1+10+40s^{-1.1}+I_{x_2}s^{-2}}$

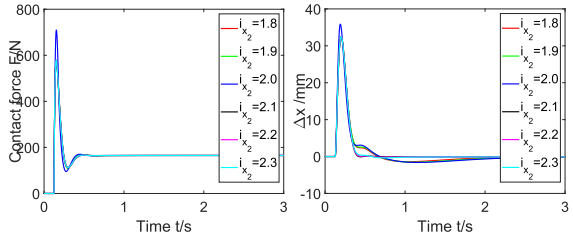

(i) Model 9: $\frac{1}{0.002s^2+0.6s^1+10+40s^{-1.1}+0.001s^{-ix_2}}$

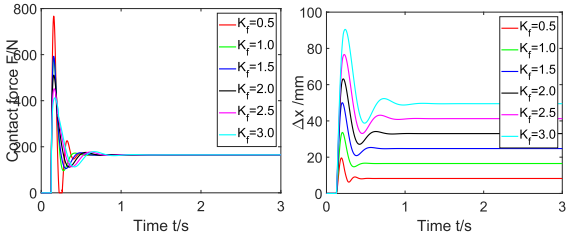

(j) Model 10: $\frac{K_f}{0.002s^2+0.6s^1+10}$

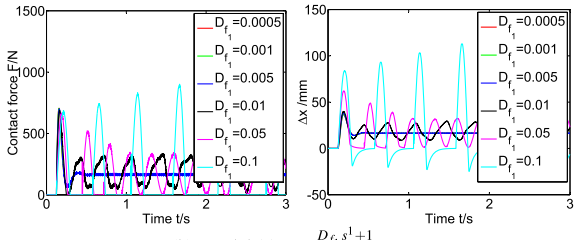

(k) Model 11: $\frac{D_{f1}s^1+1}{0.002s^2+0.6s^1+10}$

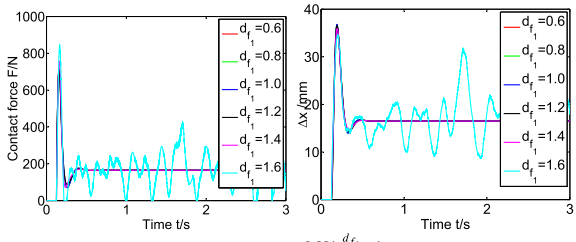

(l) Model 12: $\frac{0.001s^{d_{f1}}+1}{0.002s^2+0.6s^1+10}$

FIGURE 4. ***(Continued.)*** **The influences of parameters in (23): Model 6∼9.**

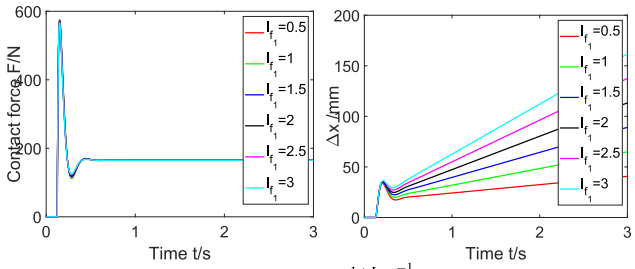

(m) Model 13: $\frac{1+I_{f1}s^{-1}}{0.002s^2+0.6s^1+10}$

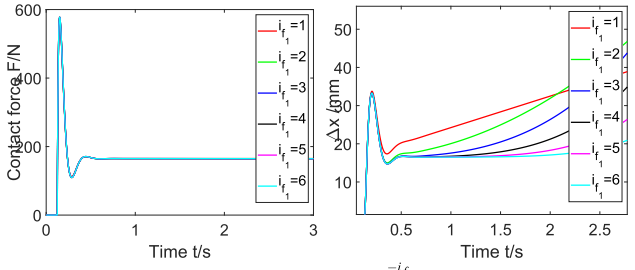

(n) Model 14: $\frac{1+0.5s^{-if_1}}{0.002s^2+0.6s^1+10}$

FIGURE 4. ***(Continued.)*** **The influences of parameters in (23): Model 10∼14.**

to behave like a stiffness so that the system energy cannot be dissipated well and no stable state can be reached. When $d_{x_1} \in [0.9, 1.1]$, a good transition can be obtained.

3) Model 3: $\frac{1}{0.6s^1+K_x}$
K_x is the traditional stiffness in (16). A large K_x leads to a small tracking error. And, an appropriate K_x should be chosen or K_x should be tuned to minimize the contact force.
4) Model 4: $\frac{1}{D_{x_2}s^2+0.6s^1+10}$
D_{x_2} is the traditional inertia in (16). A large D_{x_2} causes a large contact force and attenuated oscillations until the system comes into a stable state.
5) Model 5: $\frac{1}{0.002_2s^{d_{X_2}}+0.6_1s^1+10}$
When d_{x_2} closes to 1.5, the inertia-like D_{x_2} begins to behave damping-like. When d_{x_2} grows, an oscillation will occur in the first compression.
6) Model 6: $\frac{1}{0.002s^2+0.6s^1+10+I_{x_1}s^{-1}}$
The novelty is that a suitable I_{x_1} can be utilized to eliminate the tracking error. A small I_{x_1} has a long converge time, while a large one will cause oscillations before the system comes into a stable state.
7) Model 7: $\frac{1}{0.002s^2+0.6s^1+10+40s^{-ix_1}}$
The i_{x_1} mainly affects the transition of contact force and tracking error, but it has little effect on their values. When i_{x_1} closes to 0, I_{x_1} behaves like a stiffness. When i_{x_1} closes to 1.5, an overshoot/oscillation forms.
8) Model 8: $\frac{1}{0.002s^2+0.6s^1+10+40s^{-1.1}+I_{x_2}s^{-2}}$
The I_{x_2} mainly affects the transition of tracking error, but it has little effect on the contact force. A large I_{x_2}

leads to large oscillations before the system comes into a stable state.

9) Model 9: $\frac{1}{0.002s^2+0.6s^1+10+40s^{-1.1}+0.001s^{-i_{x_2}}}$
The i_{x_2} mainly affects the transition of tracking error, but it has little effect on the contact force. Both a small and large i_{x_2} will cause oscillations before the system comes into a stable state. Nothing that the difference in $i_{x_2} = 2.0$ with Model 8 results from the approximation of fractional order.
10) Model 10: $\frac{K_f}{0.002s^2+0.6s^1+10}$
The K_f (in numerator) is another form of traditional stiffness in (16). A large K_f leads to a large tracking error. And, an appropriate K_f should be chosen or K_f should be tuned to minimize the contact force.
11) Model 11: $\frac{D_{f_1}s^1+1}{0.002s^2+0.6s^1+10}$
When D_{f_1} grows, oscillations will occur. The energy is added into system so that the system begins to bouncing up with the growing D_{f_1}. The dissipated energy is fixed by the chosen damping 0.6, while the added energy depends on D_{f_1}.
12) Model 12: $\frac{0.001s^{d_{f_1}}+1}{0.002s^2+0.6s^1+10}$
When d_{f_1} closes to 0, D_{f_1} begins to behave like K_f. When d_{f_1} grows, undesired oscillations will occur.
13) Model 13: $\frac{1+I_{f_1}s^{-1}}{0.002s^2+0.6s^1+10}$
The I_{f_1} mainly affects the tracking error, but it has little effect on the contact force. The increasing speed of tracking error grows with the increasing I_{f_1}.
14) Model 14: $\frac{1+0.5s^{-i_{f_1}}}{0.002s^2+0.6s^1+10}$
The i_{f_1} mainly affects the tracking error, but it has little effect on the contact force. When i_{f_1} closes to 0, I_{f_1} begins to behave like K_f. Actually, i_{f_1} is the increasing speed exponent of tracking error.

Based on the above simulation results and compared with traditional impedance control, the proposed novel fractional order impedance control has little effect on reducing contact impact F_e, but it can improve the transition process of force/position response efficiently and decrease the tracking error $\Delta x = x_d - x$ gradually.

B. COMPARATIVE SIMULATIONS

Comparative simulations of hydraulic bouncing system in a free falling situation with an initial height $H = 160mm$ were done in four different impedance models. As shown in Fig. 5, the left figure is a picture of simulation video, the middle figure shows the contact force of system with respect to time, and the right figure shows the displacement control of cylinder with respect to time. Noting that the stroke of cylinder is not limited in the simulations. Fig. 5(a) and 5(b) are the traditional ($\frac{1}{0.6s^1+10}$) and proposed fractional order ($\frac{1}{0.002s^{1.9}+0.6s^{0.95}+10+40s^{-1.1}}$) impedance model, respectively. These two models are both energy dissipating impedance model and the proposed fractional order impedance control is with an added integral item, which could eliminate the tracking error and achieve more significant compliance behavior.

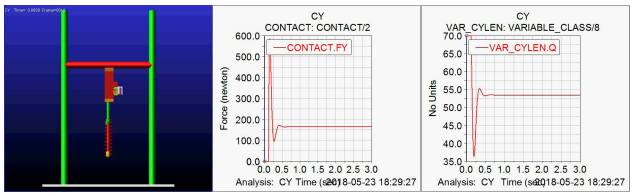

(a) Traditional impedance model: $\frac{1}{0.6s^1+10}$ https://youtu.be/h5uBiMIziJU

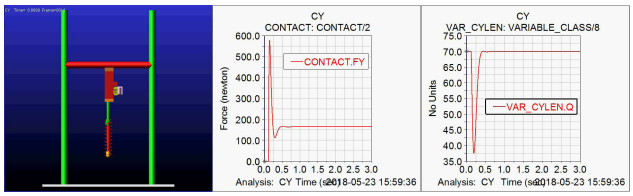

(b) Fractional order impedance model: $\frac{1}{0.002s^{1.9}+0.6s^{0.95}+10+40s^{-1.1}}$ https://youtu.be/UMgfV7xIIxk

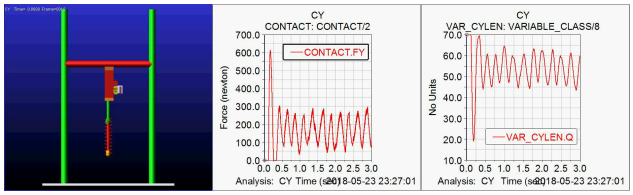

(c) Energy holding impedance model: $\frac{1}{0.6s^{0.7}+10}$ https://youtu.be/g4LbhrrdmJI

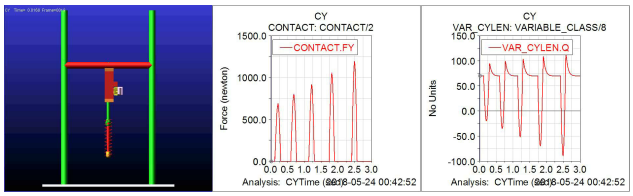

(d) Energy absorbing impedance model: $\frac{0.1s^1+1}{0.002s^2+0.6s^1+10}$ https://youtu.be/DE9X5q4W3dI

FIGURE 5. Comparative simulations.

Fig. 5(c) and 5(d) are the energy holding ($\frac{1}{0.6s^{0.7}+10}$) and absorbing ($\frac{0.1s^1+1}{0.002s^2+0.6s^1+10}$) impedance model, which provide guides for legged robots on bouncing height control and jumping control, respectively.

In order to know why more significant compliant behavior can be achieved in the proposed novel fractional order impedance control, the further research of comparative simulations are implemented in Fig. 5 and their calculated stiffness and damping of four impedance models are shown in Fig. 6. In Fig. 6(a), easy to see that the calculated stiffness and damping are almost the same to the given ones $K_x = 10N/mm$, $D_{x_1} = 0.6Ns/mm$ in the traditional impedance model ($\frac{1}{0.6s^1+10}$). In Fig. 6(b), the calculated stiffness and damping are variable in impact phase in the fractional order impedance model ($\frac{1}{0.002s^{1.9}+0.6s^{0.95}+10+40s^{-1.1}}$). This result validates references [9], [10], and it is also the reason why more significant compliant behavior can be achieved. Besides, the calculated values of stiffness and damping would

decrease to be negative in compressing phase and increase to be positive again in rebounding phase. As thus, the system energy could be dissipated more efficiently so that the system could reach a stable state faster without oscillations. In Fig. 6(c), the calculated damping doesn't change a lot in the energy holding impedance model ($\frac{1}{0.6s^{0.7}+10}$), but the calculated stiffness increases in compressing phase and decreases in rebounding phase and the whole system energy is held so that the bouncing height could be kept. In Fig. 6(d), the calculated stiffness increases in compressing phase and decreases in rebounding phase in the energy absorbing impedance model ($\frac{0.1s^1+1}{0.002s^2+0.6s^1+10}$) as well, but the calculated damping always decreases from positive to negative to inject energy into the system so that the system could start to jump. Note that the calculated stiffness and damping are based on the assumption that they are the same in the neighboring two control cycles and do not change in the flight phase.

C. THE CRITERIONS OF CHOOSING AND TUNING PARAMETERS

As for robots and manipulators, three criterions are proposed as follows to choose and tune the parameters in (23).

- Firstly, the chosen parameters in (23) should guarantee the system stability. Assume the position servo controller (inner position loop in Fig. 3) is stable. If the proposed novel fractional order impedance model in (23) is stable, the whole system will stable. Our previous published work [56], [57] and literature [30], [58], [59] can be employed to ensure the stability of proposed novel fractional order impedance model in (23).
- Secondly, the parameters in (23) are chosen and tuned to make sure the contact force as small as possible. Meanwhile, the required/unrequired tracking error should have a better transition or be eliminated to tackle tasks. Therefore, model $\frac{1}{0.002s^2+0.6s^1+10+40s^{-1.1}}$ could be a better reference in Model 7.
- The detailed procedure of choosing and tuning parameters in (23) refers to *Section* IV-A. Specially, $D_{x_1}, d_{x_1}, K_x, I_{x_1}, i_{x_1}, D_{f_1}, d_{f_1}, K_f$ play more important roles among the 14 parameters in (23) and should be determined firstly.

Remark 1: To analyze the stability of proposed fractional order impedance control, the diagram of position/force based active compliance controller based on fractional order impedance control in Fig. 3 can be simplified as the last diagram of Fig. 7. The first diagram in Fig. 7 is the traditional PID control. The second diagram in Fig. 7 is the classic FOPID control. The third diagram in Fig. 7 is the traditional impedance control based position servo control. As known to us, the stability of the former three control diagrams have been proved in many published papers [39], [60] and the stability proof of the last control diagram is similar to the third one. The closed-loop transfer function of the simplified diagram of position/force based active compliance controller based on fractional order impedance control in the last

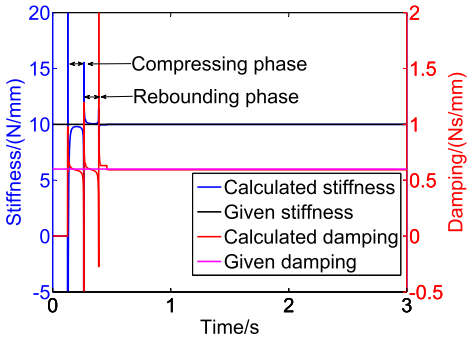

(a) Traditional impedance model: $\frac{1}{0.6s^1+10}$

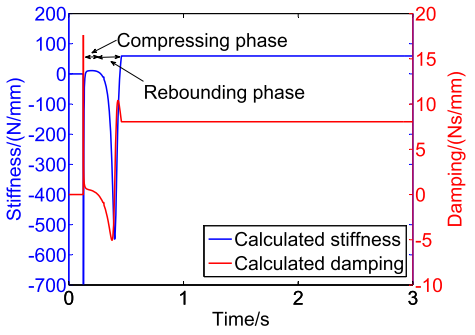

(b) Fractional order impedance model: $\frac{1}{0.002s^{1.9}+0.6s^{0.95}+10+40s^{-1.1}}$

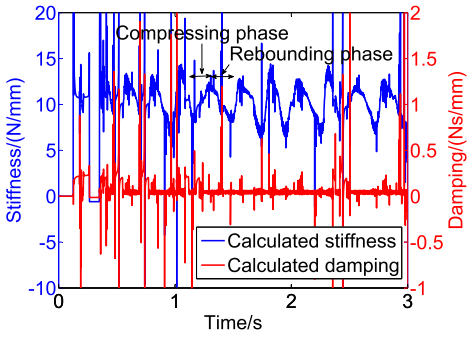

(c) Energy holding impedance model: $\frac{1}{0.6s^{0.7}+10}$

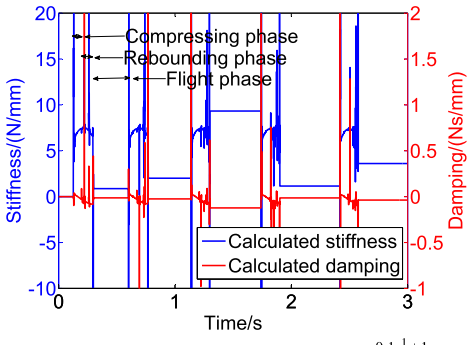

(d) Energy absorbing impedance model: $\frac{0.1s^1+1}{0.002s^2+0.6s^1+10}$

FIGURE 6. Calculated stiffness and damping.

diagram of Fig. 7 can be written as

$$\frac{F_e(s)}{x_d(s)} = \frac{C(s)S(s)}{1 + C(s)S(s)Z_{FOIM}(s)} \tag{24}$$

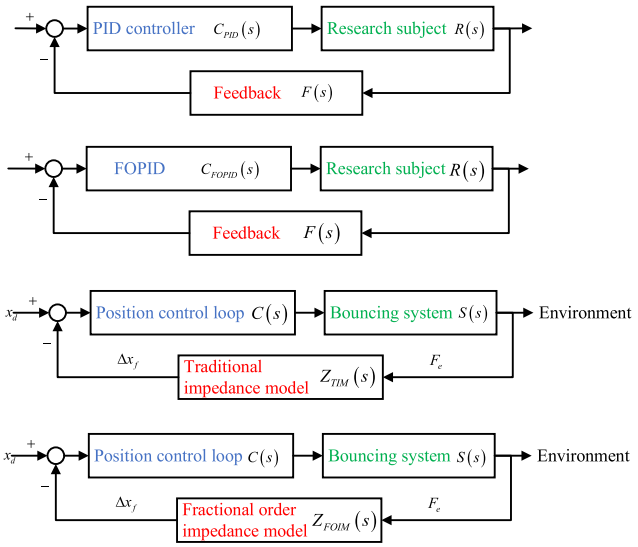

FIGURE 7. The simplified diagram of position/force based active compliance controller based on fractional order impedance control and its stability analysis.

Then its stability can be proved by root locus method, Routh criterion and Nyquist criterion in control theory. Due to the limitation of paper length, more detailed proofs about stability can be obtained in the literature [30], [56]–[59].

In addition, an adaptive method, a estimator or a observer can be used to deal with the problem of parameter uncertainties and modelling errors [47], [49], [50]. A low pass filter can be used to deal with the measurement noise and solve the robustness problem [30]. And the method in the literature [61] can be used to deal with the transmission delay problem.

Remark 2: In robotic control, legged robots are often controlled to move with small contact forces to guarantee the friendly environmental interaction and avoid large impacts to the robot bodies, which will cause robot oscillations and lead to unstable moving. Meanwhile, the robots should have a good enough performance of position tracking to tackle tasks well. Thus, the second criterion is proposed. Take Model 6 & 7 as two examples. As shown in Fig. 4(f) & Fig. 4(g), it can be found that there is not a big difference in the contact force when I_{x_2} or i_{x_2} is changing. However, there is a better tracking performance when $I_{x_2} = 40$ in Model 6 or when $i_{x_2} = 1.1$ in Model 7. That's why $I_{x_2} = 40$ has a better response in Model 6 and $i_{x_2} = 1.1$ has a better response in Model 7. This is one guide for choosing and tuning parameters in (23).

Remark 3: In practical applications, the fractional order impedance model: $\frac{1}{0.002s^{1.9}+0.6s^{0.95}+10+40s^{-1.1}}$ in Fig. 5(b) can be used to replace the traditional impedance model: $\frac{1}{0.6s^{1}+10}$ in Fig. 5(a) to eliminate the tracking error and achieve more significant compliant performance. The energy holding impedance model: $\frac{1}{0.6s^{0.7}+10}$ in Fig. 5(c) can be used to control the robots to bounce at given heights. The energy absorbing impedance model: $\frac{0.1s^{1}+1}{0.002s^{2}+0.6s^{1}+10}$ in Fig. 5(d) can be used to control the robots to jump on high platforms or over high obstacles. As for the other parameters in (23), they are can be employed based on the detailed requirements of robotic environmental interactions, as shown in Fig. 4. For example, the energy dissipating impedance models in Fig. 4 can be used to decrease the motion speed of robots, the energy holding impedance models in Fig. 4 can be used to keep the motion speed of robots, and the energy absorbing impedance models in Fig. 4 can be used to increase the motion speed of robots. Furthermore, all these 14 parameters (23) can be adaptive for robot to adapt the complicated situations that robots will meet. This is the insight this paper provides for robot dynamic interaction, bouncing and jumping control.

V. CONCLUSION

In this paper, a novel fractional order impedance control was proposed by combining an integral item and fractional order into the traditional impedance control.

Firstly, a hydraulic bouncing system was chosen as the research subject to be the simple equivalent model for studying robot dynamic interactions.

Secondly, the mathematical foundations for fractional order and traditional impedance control (position/force based active compliance controller) were given out. Synthesizing their advantages and disadvantages, the novel fractional order impedance control was proposed to improve the tracking error and contact performance. An integral item is added into the traditional impedance model to eliminate the tracking error caused by the compliant behavior. The idea of fractional order is introduced to make the orders of inertia, damping, and stiffness change from integers to fractions so that more significant compliant performance can be achieved.

Finally, comparative simulations were implemented to investigate the influence of each parameter in the proposed novel fractional order impedance model (23) and validate the efficiency of proposed method. Meanwhile, three criterions of choosing and tuning all these 14 parameters were given out.

Actually, one leg of robot can be equivalent to a hydraulic bouncing system. Thus, the research of this paper provides an insight for the compliance control for legged robots and future works will focus on the fast and high dynamic locomotion control for legged robots based on compliance control.

REFERENCES

[1] M. Vukobratovic, *Dynamics and Robust Control of Robot-Environment Interaction*, vol. 2. Singapore: World Scientific, 2009.

[2] A. Wu and H. Geyer, "The 3-D spring–mass model reveals a time-based deadbeat control for highly robust running and steering in uncertain environments," *IEEE Trans. Robot.*, vol. 29, no. 5, pp. 1114–1124, Oct. 2013.

[3] R. Nasiri, M. Khoramshahi, M. Shushtari, and M. N. Ahmadabadi, "Adaptation in variable parallel compliance: Towards energy efficiency in cyclic tasks," *IEEE/ASME Trans. Mechatronics*, vol. 22, no. 2, pp. 1059–1070, Apr. 2017.

[4] F. Angelini, G. Xin, W. J. Wolfslag, C. Tiseo, M. Mistry, M. Garabini, A. Bicchi, and S. Vijayakumar, "Online optimal impedance planning for legged robots," in *Proc. IEEE/RSJ Int. Conf. Intell. Robots Syst. (IROS)*, Nov. 2019, pp. 1–8.

[5] G. Chen, J. Wang, and L. Wang, "Gait planning and compliance control of a biped robot on stairs with desired ZMP," *IFAC Proc. Volumes*, vol. 47, no. 3, pp. 2165–2170, 2014.
[6] C. Guangrong, W. Junzheng, Z. Jiangbo, M. Liling, and S. Wei, "Stable impedance control of a single leg of hydraulic legged robot based on virtual decomposition control," *Robot*, vol. 39, no. 5, pp. 704–714, 2017.
[7] N. Hogan, "Impedance control: An approach to manipulation: Part I—Theory," *J. Dyn. Sys., Meas., Control*, vol. 107, no. 1, pp. 1–7, Mar. 1985.
[8] T. Boaventura, G. A. Medrano-Cerda, C. Semini, J. Buchli, and D. G. Caldwell, "Stability and performance of the compliance controller of the quadruped robot HyQ," in *Proc. IEEE/RSJ Int. Conf. Intell. Robots Syst.*, Nov. 2013, pp. 1458–1464.
[9] Z. Shen and J. Seipel, "The leg stiffnesses animals use may improve the stability of locomotion," *J. Theor. Biol.*, vol. 377, pp. 66–74, Jul. 2015.
[10] Z. Shen and J. Seipel, "Animals prefer leg stiffness values that may reduce the energetic cost of locomotion," *J. Theor. Biol.*, vol. 364, pp. 433–438, Jan. 2015.
[11] Z. Wang, H. M. Yip, D. Navarro-Alarcon, P. Li, Y.-H. Liu, D. Sun, H. Wang, and T. H. Cheung, "Design of a novel compliant safe robot joint with multiple working states," *IEEE/ASME Trans. Mechatronics*, vol. 21, no. 2, pp. 1193–1198, Apr. 2016.
[12] Y. Liu, Y. Zhang, and Q. Xu, "Design and control of a novel compliant constant-force gripper based on buckled fixed-guided beams," *IEEE/ASME Trans. Mechatronics*, vol. 22, no. 1, pp. 476–486, Feb. 2017.
[13] C. Semini, V. Barasuol, T. Boaventura, M. Frigerio, and J. Buchli, "Is active impedance the key to a breakthrough for legged robots?" in *Robotics Research*. Cham, Switzerland: Springer, 2016, pp. 3–19.
[14] D. Yamada, J. Huang, and T. Yabuta, "Comparison between admittance and impedance control of a multi-finger-arm robot using the guaranteed manipulability method," *Precis. Instrum. Mechanol.* vol. 2, no. 1, pp. 85–93, 2013.
[15] C. Ott, R. Mukherjee, and Y. Nakamura, "Unified impedance and admittance control," in *Proc. IEEE Int. Conf. Robot. Autom.*, May 2010, pp. 554–561.
[16] E. Rivet, S. Karkar, and H. Lissek, "Broadband low-frequency electroacoustic absorbers through hybrid sensor-/shunt-based impedance control," *IEEE Trans. Control Syst. Technol.*, vol. 25, no. 1, pp. 63–72, Jan. 2017.
[17] Y. Li and S. S. Ge, "Impedance learning for robots interacting with unknown environments," *IEEE Trans. Control Syst. Technol.*, vol. 22, no. 4, pp. 1422–1432, Jul. 2014.
[18] I. Ranatunga, F. L. Lewis, D. O. Popa, and S. M. Tousif, "Adaptive admittance control for human–robot interaction using model reference design and adaptive inverse filtering," *IEEE Trans. Control Syst. Technol.*, vol. 25, no. 1, pp. 278–285, Jan. 2017.
[19] Y. Aydin, O. Tokatli, V. Patoglu, and C. Basdogan, "Stable physical human-robot interaction using fractional order admittance control," *IEEE Trans. Haptics*, vol. 11, no. 3, pp. 464–475, Jul. 2018.
[20] B.-P. Huynh, C.-W. Wu, and Y.-L. Kuo, "Force/position hybrid control for a hexa robot using gradient descent iterative learning control algorithm," *IEEE Access*, vol. 7, pp. 72329–72342, 2019.
[21] S. Xu, B. He, Y. Zhou, Z. Wang, and C. Zhang, "A hybrid position/force control method for a continuum robot with robotic and environmental compliance," *IEEE Access*, vol. 7, pp. 100467–100479, 2019.
[22] H. Navvabi and A. H. D. Markazi, "Hybrid position/force control of stewart manipulator using extended adaptive fuzzy sliding mode controller (E-AFSMC)," *ISA Trans.*, vol. 88, pp. 280–295, May 2019.
[23] M. Vukobratovic and Y. Ekalo, "Unified approach to control laws synthesis for robotic manipulators in contact with dynamic environment," in *Proc. Tutorial S5, Force Contact Control Robotic Syst., IEEE Int. Conf. Robot. Autom.*, May 1993, pp. 213–229.
[24] O. Khatib, "A unified approach for motion and force control of robot manipulators: The operational space formulation," *IEEE J. Robot. Autom.*, vol. 3, no. 1, pp. 43–53, Feb. 1987.
[25] T. Lin and A. A. Goldenberg, "A unified approach to motion and force control of flexible joint robots," in *Proc. IEEE Int. Conf. Robot. Autom.*, vol. 2, Apr. 1996, pp. 1115–1120.
[26] K.-X. Ba, B. Yu, G.-L. Ma, Q.-X. Zhu, Z.-J. Gao, and X.-D. Kong, "A novel position-based impedance control method for bionic legged Robots' HDU," *IEEE Access*, vol. 6, pp. 55680–55692, 2018.
[27] M. Focchi, "Strategies to improve the impedance control performance of a quadruped robot," Ph.D. dissertation, Dept. Dyn. Legged Syst. Lab, Istituto Italiano di Tecnologia, Univ. Genova, Italy, 2013.
[28] S. Jung, T. C. Hsia, and R. G. Bonitz, "Force tracking impedance control of robot manipulators under unknown environment," *IEEE Trans. Control Syst. Technol.*, vol. 12, no. 3, pp. 474–483, May 2004.
[29] D. Valério and J. S. Da Costa, *An Introduction to Fractional Control*, vol. 91. Edison, NJ, USA: IET, 2013.
[30] S. Oh and Y. Hori, "Realization of fractional order impedance by feedback control," in *Proc. 33rd Annu. Conf. IEEE Ind. Electron. Soc. (IECON)*, Nov. 2007, pp. 299–304.
[31] S. Oh and Y. Hori, "Fractional order impedance control by particle swarm optimization," in *Proc. Int. Conf. Control, Autom. Syst.*, Oct. 2008, pp. 1936–1941.
[32] Y. Chen, J. Zhao, J. Wang, and D. Li, "Fractional-order impedance control for a wheel-legged robot," in *Proc. 29th Chin. Control Decis. Conf. (CCDC)*, May 2017, pp. 7845–7850.
[33] C. Ding, J. Cao, and Y. Chen, "Fractional-order model and experimental verification for broadband hysteresis in piezoelectric actuators," *Nonlinear Dyn.*, vol. 98, no. 4, pp. 3143–3153, Dec. 2019.
[34] C. I. Muresan, S. Folea, I. R. Birs, and C. Ionescu, "A novel fractional-order model and controller for vibration suppression in flexible smart beam," *Nonlinear Dyn.*, vol. 93, no. 2, pp. 525–541, Jul. 2018.
[35] Y. Chen, B. M. Vinagre, and I. Podlubny, "Continued fraction expansion approaches to discretizing fractional order derivatives—An expository review," *Nonlinear Dyn.*, vol. 38, nos. 1–4, pp. 155–170, Dec. 2004.
[36] R. Herrmann, *Fractional Calculus: An Introduction for Physicists*, 3rd ed. Singapore: World Scientific, 2018.
[37] M. D. Ortigueira, *Fractional Calculus for Scientists and Engineers*, vol. 84. London, U.K.: Springer, 2011.
[38] R. L. Magin, *Fractional Calculus in Bioengineering*, vol. 2. Redding, CA, USA: Begell House, 2006.
[39] C. A. Monje, Y. Chen, B. M. Vinagre, D. Xue, and V. Feliu-Batlle, "Fractional-order systems and controls: Fundamentals and applications," Springer Science & Business Media (2010).
[40] H. Delavari, R. Ghaderi, A. Ranjbar, and S. Momani, "Fuzzy fractional order sliding mode controller for nonlinear systems," *Commun. Nonlinear Sci. Numer. Simul.*, vol. 15, no. 4, pp. 963–978, Apr. 2010.
[41] B. Vinagre, I. H. A. Podlubny, and V. Feliu, "Some approximations of fractional order operators used in control theory and applications," *Fractional Calculus Appl. Anal.*, vol. 3, no. 3, pp. 231–248, 2000.
[42] A. Oustaloup, F. Levron, B. Mathieu, and F. M. Nanot, "Frequency-band complex noninteger differentiator: Characterization and synthesis," *IEEE Trans. Circuits Syst. I, Fundam. Theory Appl.*, vol. 47, no. 1, pp. 25–39, Jan. 2000.
[43] G. Chen, J. Wang, S. Wang, J. Zhao, and W. Shen, "Compliance control for a hydraulic bouncing system," *ISA Trans.*, vol. 79, pp. 232–238, Aug. 2018.
[44] M. M. Ankarali and U. Saranli, "Stride-to-stride energy regulation for robust self-stability of a torque-actuated dissipative spring-mass hopper," *Chaos: Interdiscipl. J. Nonlinear Sci.*, vol. 20, no. 3, Sep. 2010, Art. no. 033121.
[45] P. Terry and K. Byl, "An analytically computable model and energy-based control for a realistic series-elastic 1D hopper on rough terrain," in *Proc. Intell. Robots Syst. (IROS)*, 2014, p. 1.
[46] G. Chen, J. Wang, S. Wang, J. Zhao, W. Shen, and J. Li, "Application of a new adaptive robust controller design method to electro-hydraulic servo system," *Acta Automatica Sinica*, vol. 42, no. 3, pp. 375–384, 2016.
[47] G. Chen, J. Wang, L. Ma, and R. Hao, "Observer-based and energy saving control of single-rod electro-hydraulic servo system driven by servo motor," in *Proc. Amer. Control Conf. (ACC)*, Jul. 2015, pp. 2224–2229.
[48] G. Chen, J. Wang, S. Wang, and L. Ma, "Separate meter in and separate meter out energy saving control system using dual servo valves under complex load conditions," *Trans. Beijing Inst. Technol.*, vol. 36, no. 10, pp. 1053–1058, 2016.
[49] G. Chen, J. Wang, S. Wang, J. Zhao, and W. Shen, "Indirect adaptive robust dynamic surface control in separate meter-in and separate meter-out control system," *Nonlinear Dyn.*, vol. 90, no. 2, pp. 951–970, Oct. 2017.
[50] G. Chen, J. Wang, S. Wang, J. Zhao, and W. Shen, "Energy saving control in separate meter in and separate meter out control system," *Control Eng. Pract.*, vol. 72, pp. 138–150, Mar. 2018.
[51] G. Chen, J. Wang, L. Wang, and Y. He, "Design and simulation of a hydraulic biped robot," in *Proc. 32nd Chin. Control Conf. (CCC)*, Jul. 2013, pp. 4244–4249.
[52] T.-Y. Choi, B.-S. Choi, and K.-H. Seo, "Position and compliance control of a pneumatic muscle actuated manipulator for enhanced safety," *IEEE Trans. Control Syst. Technol.*, vol. 19, no. 4, pp. 832–842, Jul. 2011.

[53] R. Magin, M. D. Ortigueira, and I. T. J. Podlubny, "On the fractional signals and systems," *Signal Process.*, vol. 91, no. 3, pp. 350–371, 2011.
[54] M. Ortigueira and J. Machado, "Which derivative?" *Fractal Fractional*, vol. 1, no. 1, pp. 1–13, 2017.
[55] A. Carpinteri and F. Mainardi, *Fractals and Fractional Calculus in Continuum Mechanics*, vol. 378. New York, NY, USA: Springer-Verlag Wien, 2014.
[56] Z. Jiangbo and W. Junzheng, "The fractional order PI control for an energy saving electro-hydraulic system," *Trans. Inst. Meas. Control*, vol. 39, no. 4, pp. 505–519, Apr. 2017.
[57] J. Zhao, J. Wang, and S. Wang, "Fractional order control to the electro-hydraulic system in insulator fatigue test device," *Mechatronics*, vol. 23, no. 7, pp. 828–839, Oct. 2013.
[58] Y. Li, Y. Chen, and I. Podlubny, "Mittag–Leffler stability of fractional order nonlinear dynamic systems," *Automatica*, vol. 45, no. 8, pp. 1965–1969, Aug. 2009.
[59] Y. Li, Y. Chen, and I. Podlubny, "Stability of fractional-order nonlinear dynamic systems: Lyapunov direct method and generalized Mittag–Leffler stability," *Comput. Math. Appl.*, vol. 59, no. 5, pp. 1810–1821, Mar. 2010.
[60] J. Koivumaki and J. Mattila, "Stability-guaranteed impedance control of hydraulic robotic manipulators," *IEEE/ASME Trans. Mechatronics*, vol. 22, no. 2, pp. 601–612, Apr. 2017.
[61] X. Yang, Q. Song, Y. Liu, and Z. Zhao, "Finite-time stability analysis of fractional-order neural networks with delay," *Neurocomputing*, vol. 152, pp. 19–26, Mar. 2015.

GUANGRONG CHEN received the B.Eng. degree in automation and the Ph.D. degree in control science and engineering from the Beijing Institute of Technology, Beijing, China, in 2012 and 2018, respectively. He joined the Robotics Research Center, Beijing Jiaotong University, as a Lecturer, in 2018. His research interests include robotic control, nonlinear systems, and adaptive control.

SHENG GUO received the Ph.D. degree from Beijing Jiaotong University, in 2005. He was a Postdoctoral Researcher with National Cheng Kung University, from 2005 to 2006. He was a Visiting Scholar with the University of California, Irvine, USA, from 2010 to 2011. He is currently a Full Professor with Beijing Jiaotong University, the Vice Director of the Robotics Institute, Beijing Jiaotong University, and the Vice Dean of the School of Mechanical, Electronic and Control Engineering, Beijing Jiaotong University. His research interests include robotics mechanism and mechatronics.

BOWEN HOU received the Ph.D. degree from Beijing Jiaotong University, in 2016. He was a Postdoctoral Researcher with Beijing Jiaotong University, from 2016 to 2018. He was a Visiting Scholar with Heriot-Watt University in Edinburgh, U.K., from 2017 to 2018. He is currently a Lecturer with the School of Civil Engineering, Beijing Jiaotong University. His research interests include vehicle-track dynamics, environmental vibration and noise, and track dynamics in-situ measurement.

JUNZHENG WANG received the Ph.D. degree in control science and engineering from the Beijing Institute of Technology, Beijing, China, in 1994. He is currently the Deputy Director of the Key Laboratory of Intelligent Control and Decision of Complex Systems, Beijing Institute of Technology, where he is also a Professor and a Ph.D. Supervisor. His current research interests include motion control, static and dynamic performance testing of electric and electric hydraulic servo system, and dynamic target detection and tracking based on image technology. Prof. Wang is a Senior Member of the Chinese Mechanical Engineering Society and the Chinese Society for Measurement. He received the Second Award from the National Scientific and Technological Progress (No. 1), in 2011.